Available online at www.sciencedirect.com
ScienceDirect
Journal of Power Sources 167 (2007) 442–449
JOURNAL OF POWER SOURCES
www.elsevier.com/locate/jpowsour

Portable DMFC system with methanol sensor-less control

C.Y. Chen *, D.H. Liu, C.L. Huang, C.L. Chang

Institute of Nuclear Energy Research (INER), No. 1000, Wunhua Rd., Jiaan Village, Longtan Township, Taoyuan County 32546, Taiwan, ROC

Received 20 January 2007; received in revised form 16 February 2007; accepted 19 February 2007
Available online 2 March 2007

Abstract

This work develops a prototype 20 W portable DMFC by system integration of stack, condenser, methanol sensor-less control and start-up characteristics. The effects of these key components and control schemes on the performance are also discussed. To expedite the use of portable DMFC in electronic applications, the system utilizes a novel methanol sensor-less control method, providing improved fuel efficiency, durability, miniaturization and cost reduction. The operating characteristics of the DMFC stack are applied to control the fuel ejection time and period, enabling the system to continue operating even when the MEAs of the stack are deteriorated. The portable system is also designed with several features including water balance and quick start-up (in 5 min). Notably, the proposed system using methanol sensor-less control with injection of pure methanol can power the DVD player and notebook PC. The system specific energy and energy density following three days of operation are 362 Wh kg^{-1} and 335 Wh L^{-1}, respectively, which are better than those of lithium batteries (~150 Wh kg^{-1} and ~250 Wh L^{-}). This good energy storage feature demonstrates that the portable DMFC is likely to be valuable in computer, communication and consumer electronic (3C) markets.

Keywords: Direct methanol fuel cell; Membrane electrode assembly; Energy density; Power density; Methanol sensor-less control; System integration

1. Introduction

Fuel cell technology is becoming widely adopted worldwide because of its potential applications in power stations, residential power, road transportation and portable power-supply units [1–4]. Fuel cells are efficient, silent and clean energy conversion systems that produce electricity via electrochemistry [1]. A portable electronic application is considered as one of the most significant entry points for fuel cells into the commercial market. Additionally, direct methanol fuel cells (DMFC) are expected to be the first fuel cells to provide power for portable electronic devices, such as mobile phones, laptop computers and advanced mobile electronic devices [5,6], because they have many benefits over other fuel cells. These advantages include low operating temperature, rapid start-up, compactness and mass production capability, use of liquid fuel, existing supply infrastructure and fewer safety concerns when compared with proton exchange membrane fuel cells (PEMFC). However, despite this recognition of the advantages of fuel cells, mass production in fuel cells has yet started. The DMFC is likely to become a viable commercial product for portable electronics once some critical engineering challenges, such as difficulty in increasing conversion efficiency and durability together with reducing system size and cost, are eliminated. Therefore, many studies [7–18] have concentrated on DMFC. Much effort has been made on improving the MEA by modifying the Nafion membrane structure [19], designing new proton-conducting polymers [20], finding more active catalysts [21,22], optimizing electrode structures [23] or improving the stack structure design [24], to increase the power and energy density of the DMFC. However, DMFC system integration for portable applications has not been widely explored [25]. Therefore, this study integrates the DMFC system with the proposed innovative method of methanol sensor-less control, and shows that a portable 20 W DMFC can be constructed for applications in laptop computers and DVD players. The investigation focuses on stack development, methanol sensor-less control, system condenser and start-up characteristics, and includes system performance analysis to accelerate commercialization of portable DMFCs.

2. System description

The DMFC developed at the Institute of Nuclear Energy Research (INER) in Taiwan is an active system using the high

* Corresponding author. Tel.: +886 3 4711400x6653; fax: +886 3 4711409.
E-mail address: cychen@iner.gov.tw (C.Y. Chen).

0378-7753/$ – see front matter © 2007 Elsevier B.V. All rights reserved.
doi:10.1016/j.jpowsour.2007.02.056

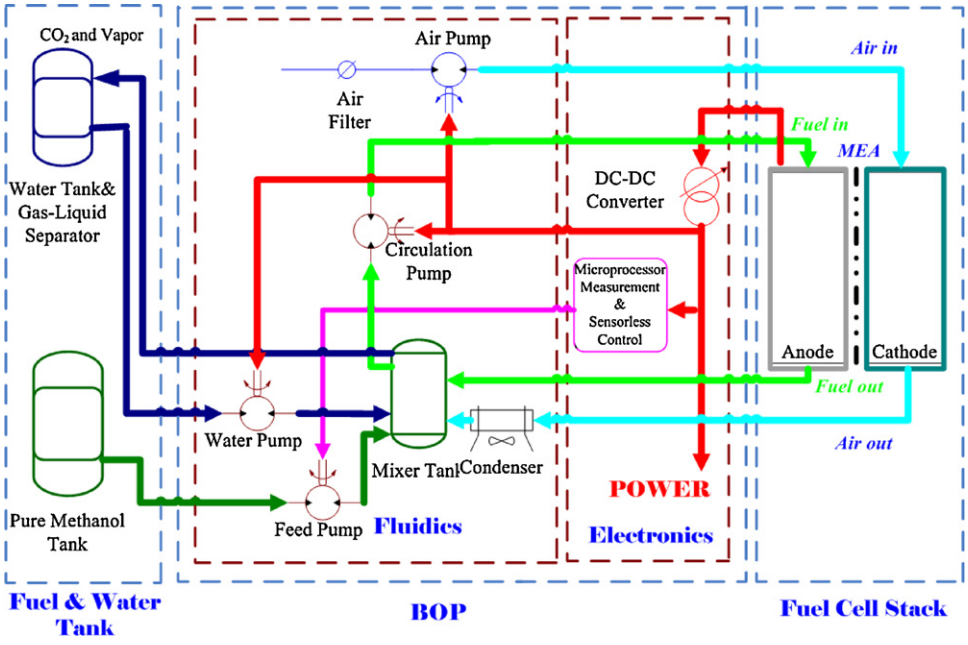

Fig. 1. The schematic diagram of the portable DMFC system.

energy density of pure methanol and methanol sensor-less control. Fig. 1 shows a schematic diagram of the portable DMFC system. To minimize the methanol crossover, the system utilizes a diluted methanol solution supplied to the anode. The methanol solution is well diluted in a container of approximately 30 mL, known as the mixing tank. The mixing tank collects the water/air mixture from the cathode, and the fuel/CO_2 mixture from the anode. The air and CO_2 are then vented into the ambient air from the mixing tank. A methanol sensor-less control method is adopted to trigger the feed pump to add a specific quantity of pure methanol to the mixing tank. The circulation pump continuously feeds the fuel from the mixing tank to the stack in a recirculation loop. The water pump feeds water from the water tank to the mixing tank in a constant period.

The anode side of the DMFC reaction needs one molecule of water for each molecule of methanol consumed. At the cathode side, O_2 from the air reacts with the protons and electrons to form water. An air pump not only supplies the required O_2 from the air to the cathode, but also forces the vapor (air + water) into the mixing tank via the condenser. The condenser system recovers water in the system. Some liquid water is condensed from the vapor, and then returned to the anode circulation loop to maintain the water balance within the system.

3. Results and discussion

The development of a small portable DMFC system including stack development, methanol sensor-less control, system condenser and start-up characteristics is described as follows. A system performance analysis is also presented.

3.1. Stack development

The stack design is based on conventional bipolar stack design as developed at Institute of Nuclear Energy Research (INER). Fig. 2 shows an experimental 18-cell bipolar plate stack. The DMFC stack was built from carbon cloths, gaskets, machined graphite bipolar plates and our house-made MEAs. The Pt–Ru and Pt loadings were ~2 and ~3.5 mg cm^{-2} in anode and cathode, respectively. The MEAs, which consist of electrodes and electrolyte membrane, were prepared by the procedure same as that reported in our previous paper [23]. The MEA was then sandwiched between carbon cloths (used as dif-

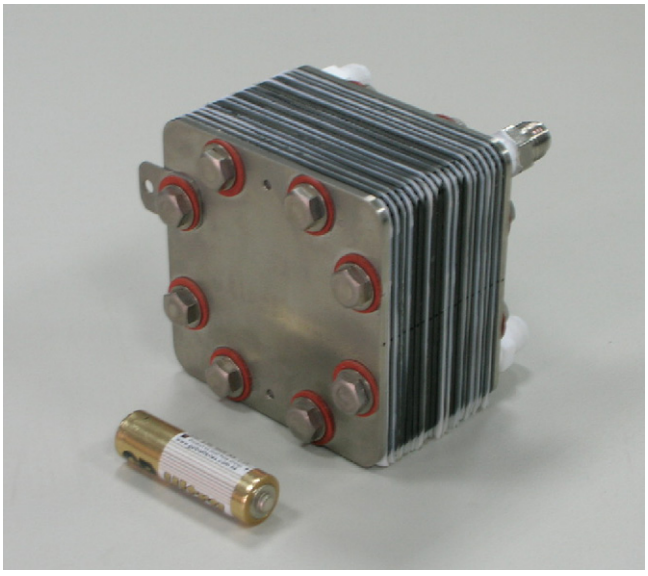

Fig. 2. An experimental 18-cell bipolar plate stack.

fusion layers) and installed in a bipolar plate stack with two current collectors positioned at each end of the stack. Teflon gaskets were placed between bipolar plates to prevent liquid and gas leakage to the exterior and cross leakage between the fluids in stack. Serpentine type flow fields were used for fuel distribution on anode and cathode sides. The current collectors were made from a stainless steel or a titanium alloy. During the development process, the stack construction was changed as a result of stack performance testing under various operating conditions.

We have built and demonstrated that the high performance of the bipolar plate stack can be obtained in a compact size suited to portable DMFCs by minimizing the thickness of the bipolar plate and increasing the number of cells in the stack. Fig. 3 shows the stack performance of 10 and 18 cells with bipolar plate thickness of 3.0 and 1.7 mm, respectively. It was demonstrated that stack power output was increased significantly from 17 to 33 W at 70 °C in air as the thickness of the bipolar plate was decreased from 3.0 to 1.7 mm and the cell number was increased from 10 to 18. Since a reduction in the bipolar plate thickness can lead to a reduction in the stack size, the volumetric power density of the stack can also be increased significantly. Fig. 4 shows that the volumetric power density of the stack at 70 °C can be increased greatly from ~60 to ~100 W L^{-1} for stacks of 10 cells (with plate thickness of 3.0 mm) and 18 cells (with plate thickness of 1.7 mm), respectively. The active area of each MEA is 25 cm^2, and the ratio of active surface area to total surface area for each cell in the stack design is about 39%. The peak power output of an 18-cell stack with bipolar plate thickness of 1.7 mm can reach 33 W with air operation at 70 °C. The stack has a total volume of about 326 cm^3 with a weight of about 700 g. In the steady state operation of constant load, the 22-cell stack was assembled for the stack output of 28 W, enabling the system to generate 20 W net power after the consumption of auxiliary power. The stack was self-heated in the system to a temperature of about 60 °C under the steady state operation. The typical stack

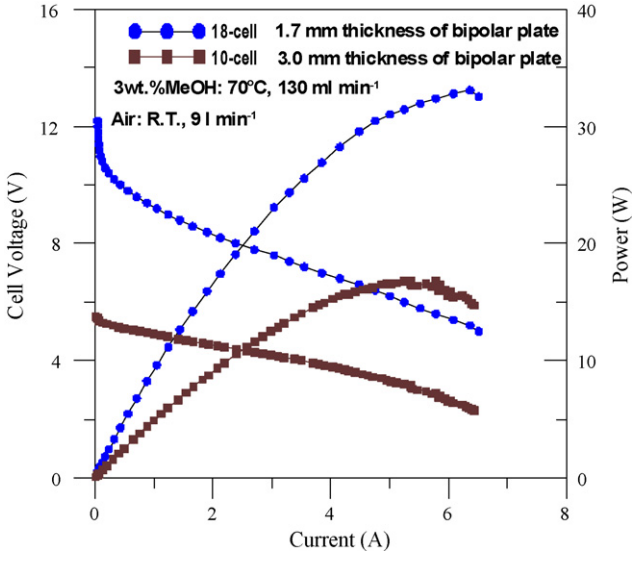

Fig. 3. Stack performance of 10- and 18-cell stacks with bipolar plate thickness of 3.0 and 1.7 mm, respectively.

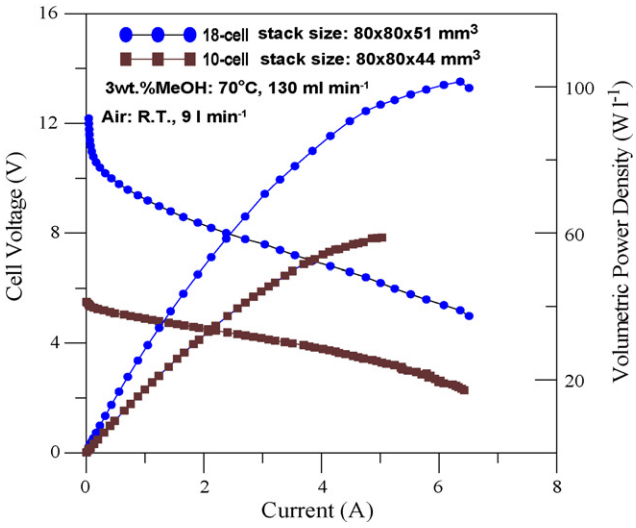

Fig. 4. Volumetric power density of 10- and 18-cell stacks with bipolar plate thickness of 3.0 and 1.7 mm, respectively.

operating voltage was about 7.7–8.0 V, i.e. ~0.35 V for each cell. A DC–DC converter was needed to obtain the required voltage for the portable electronic devices. The stack generated backpressure of about 1.4×10^4 Pa owing to the serpentine flow field design in both the anode and cathode plates. Experimental results indicate that the proposed stack design is good enough for practical applications in 15–25 W portable DMFC systems.

The flow rate of air at the cathode had a critical impact on stack performance. The peak power increased as the air flow rate increases from 6 to 12 L min^{-1}. This is because supplying air to the cathode side removes most of the water produced at the cathodes, raises the O_2 mass transport (concentration), and reduces the methanol crossover problem. By comparison, the peak power rose slowly as the flow rate of methanol solution was raised from 80 to 130 mL min^{-1}, and then changed little at a high flow rate of 200 ml min^{-1}. Therefore, the peak power was influenced more significantly by the flow rate of air than by that of the methanol solution. These findings indicate that the stack performance was affected not only by stack structure designs, but also by operating conditions. Suitable auxiliary components should be selected to operate the system based on the operating properties of the components and their relationship with the stack performance.

3.2. Methanol sensor-less control

Minimizing the volume and weight is important for portable power sources. Therefore, to simplify the design of the liquid feed fuel cell system, and decrease its cost and complexity, a novel fuel sensor-less control scheme for a liquid feed fuel cell system was developed to eliminate the need for a fuel concentration sensor. The operating characteristics of the DMFC stack are employed to control the power generating system without the need to determine the concentration of fuel. The proposed system can operate even after the degradation of MEAs. The control algorithm, called an Impulse Response based on Discrete Time Fuel Injection (IR-DTFI), is presented as follows.

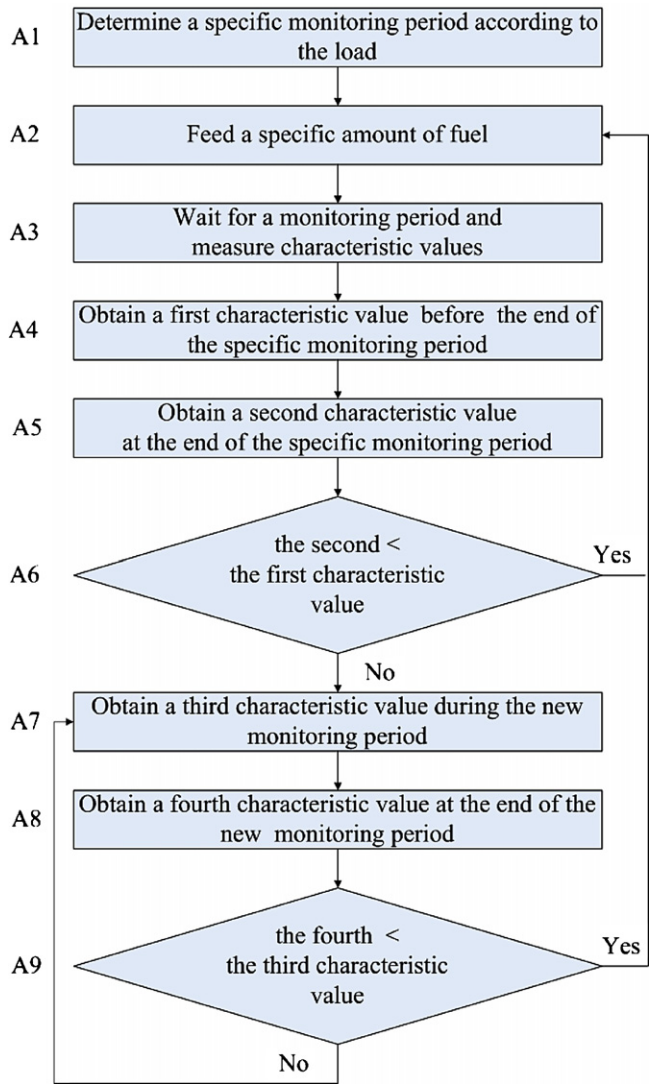

Fig. 5. Flow chart of the IR-DTFI control algorithm.

Fig. 5 shows the flow chart of the IR-DTFI strategy. Step A1 starts to determine a specific monitoring period according to the load. Fig. 6 plots the polarization curve of the fuel cell and explains how to determine the monitoring period. The power curve has a maximum power P_{max}, and the corresponding I_{max} is a suggested value for deciding the minimum duration for the

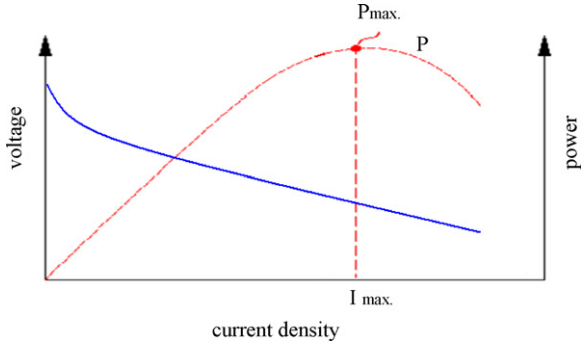

Fig. 6. Definition of P_{max} and P_{ref} by polarization curve.

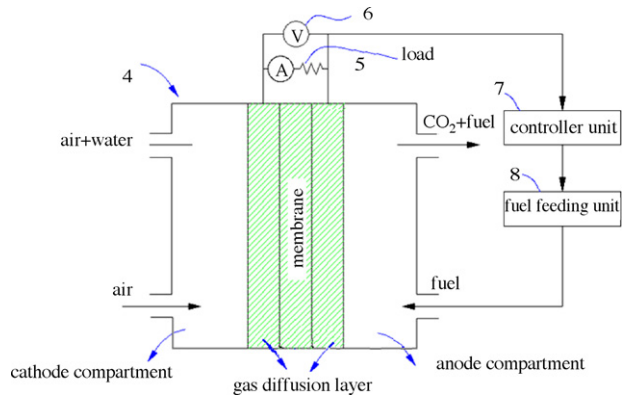

Fig. 7. Schematic diagrams of the measurement system, system control and fuel-feeding unit for the verification and evaluation of the IR-DTFI control scheme.

specific monitoring period. The system control unit determines the specific monitoring period, at any constant current discharging condition, inversely proportional to I_{max}. In addition, the minimum specific monitoring period at I_{max} is predetermined through experiment. Therefore, the specific monitoring period is the duration that the fuel cell can sustain the load (I_{max}) within the injection of a specific amount of fuel. Step A2 feeds a specific amount of fuel into the mixing tank. Fig. 7 plots the measurement system, system control and fuel-feeding unit for the verification and evaluation of the IR-DTFI control scheme.

Then, step A3 measures the operating characteristics of the fuel cell over the specific monitoring period. The operating characteristic value here can be potential, current, or power measured at the stack terminal. Step A4 obtains a first characteristic value during a time interval before the end of the specific monitoring period. Then the flow proceeds to step A5 to obtain a second characteristic value at a time point that locates at the last of the specific monitor time interval. Fig. 8(a) shows the operating characteristic obtained from the IR-DTFI control scheme. As clearly seen from trend of operating characteristic in Fig. 8(b), the system control unit should determine whether the trend of operating characteristics are going upward or downward at the end of the specific monitoring period (T_0, T_1, T_2). The relation between the first and the second characteristic value should have the capability to identify that the trend of operating characteristics is going upward or downward at the end of the specific monitoring period. From this point of view, a lot of way can define the first characteristic value. Therefore, step A6 compares the first with the second characteristic value to judge the trend. If the second is smaller than the first characteristic value that means the trend goes downward, the algorithm returns to step A2 to feed fuel to the mixing tank. It represents that the methanol concentration is insufficient for the mass transport of fuel at the end of the specific monitoring period as shown at point T_0, T_1 in Fig. 8(b).

When the trend is going upward, it means that there is excess fuel accumulated at the end of the specific monitoring period. The system control unit stops injecting fuel until the trend of operating characteristics goes downward. As shown in Fig. 8(b), the excess fuel is consumed during the injection delay period between T_2 and T_3. The methanol concentration measured at

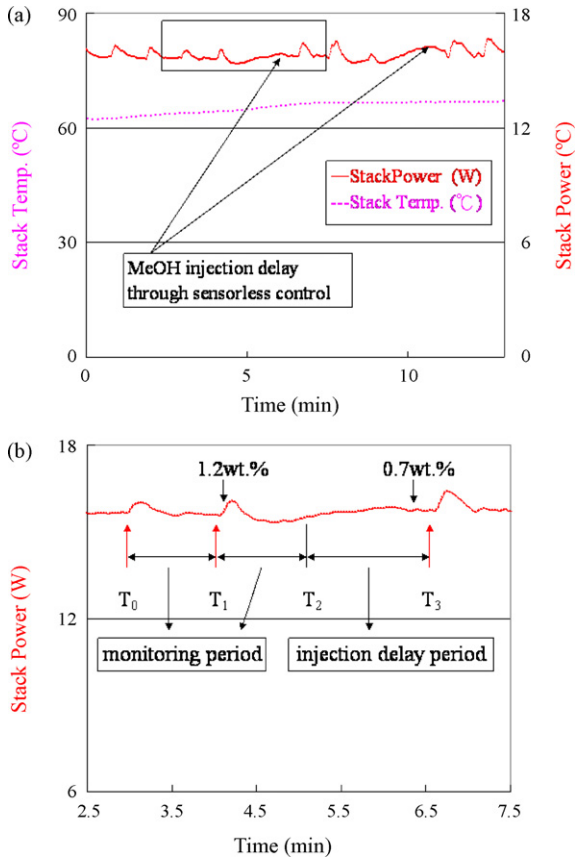

Fig. 8. (a) Operating characteristic obtained from the IR-DTFI control scheme. (b) An enlargement of the mark region in (a).

the point T_3 is about 0.7 wt.%, while the concentration measured after the injection of fuel at the point T_1 is about 1.2 wt.%. By way of the comparison method, the third and the fourth operating characteristics are set up to determine when the trend will going downward after the specific monitoring period mentioned above. If the second exceeds the first that means trend up, the flow proceeds to step A7 to calculate a third characteristic value during the new period after the specific monitoring period. Then, step A8 obtains a fourth characteristic value at the last of the new period. Step A9, then, determines whether the system control unit should feed fuel to the mixing tank. If the third exceeds the fourth that means trend down, the algorithm goes back to step A2 and system control unit signals fuel-feeding unit to inject fuel to the mixing tank. If the third is smaller than the fourth characteristic value, the algorithm returns to step A7 to explore the most recent period and to determine an updated third characteristic value. Then step A8 is repeated to determine an updated fourth characteristic value at the end of the most recent period. Again, step A9 compares the third with the fourth characteristic values. If the third exceeds the fourth, the algorithm returns to step A2 to feed fuel to the mixing tank and the whole flow start again. Through the continuous comparison process, the repeated flow steps A7–A9 aid in consuming and regulating the excess fuel accumulated in the early cycles.

When the system control unit signals to inject an amount of methanol to the mixing tank, the operating characteristics begin to go upward normally due to the increasing of methanol concentration. Meanwhile, owing to the methanol crossover, the mixed potential occurring at cathode builds up gradually and lowers the operating characteristics. As shown in Fig. 8(a), every peak is the combination of the aforementioned two effects caused by the discrete time injections of neat methanol. If the concentration is just enough, then the downward trend will approximately like a linear decay. If there is excess fuel accumulated, then the operating characteristics will go downward dramatically due to methanol crossover. With time passing away, the fuel is consumed gradually, and the mixed potential effect is reduced. Therefore, the operating characteristics will go downward, experience the minimum values and then go upward. If the trend is going upward at the end of the specific monitoring period, it means that there is excess fuel accumulated, and the system control unit stop injecting neat methanol until the excess fuel is consumed and the trend is going downward. On the contrary, if the trend is going downward at the end of the specific monitoring period, that means the fuel concentration is insufficient, then the system control unit injects the neat methanol at the same time.

The experiments through various operation modes, such as constant voltage, constant current and constant resistant modes were also conducted to verify the feasibility of this control algorithm. For more detailed description please see in our recent paper [26].

3.3. System condenser and start-up

The condenser is the most important component for controlling the water balance in the system. Table 1 compares three cooling conditions for DMFC system. The table reveals that the system without a condenser is the worst case. The water consumption rate of this system was 22.8 mL h^{-}. The exhaust temperature of the vapor was 60 °C, which is almost the same as the stack temperature. Adding a condenser cooled by a fan removed some heat, and condensed much of the vapor into liquid water. The water consumption rate of system thus decreased from 22.8 to 9.7 mL h^{-1}, indicating that the condenser condensed vapor into liquid water at a rate of 13.1 mL h^{-1}. The exhaust temperature of the vapor was also reduced from 60 to 47 °C. Moreover, the water consumption rate with the condenser outside the system box was −1.8 mL h^{-1}. The minus sign means that the amount of water increased. This improved cooling condition meant that the condenser caused more vapor to be condensed into liquid water (24.6 mL h^{-1}). The vapor temperature further fell from 47 to 42 °C follow-

Table 1
Comparison of water balance in various systems

System types	Water consuming rate (cc h^{-1})	Exhaust temperature (°C)
Without condenser	22.8	60
With condenser inside the system box	9.7	47
With condenser outside the system box	−1.8	42

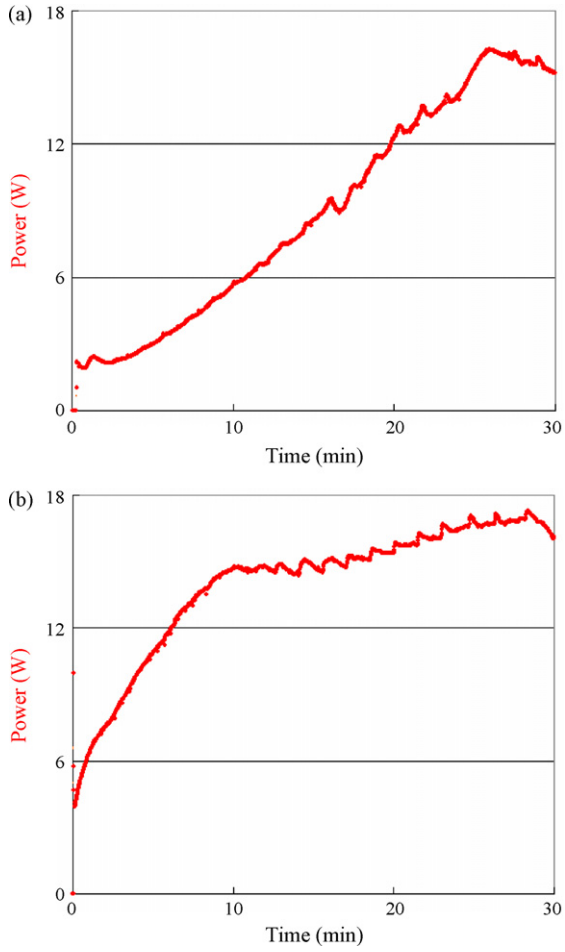

Fig. 9. Variation of start-up time with different initial methanol concentrations (a) 1 wt.%; (b) 9 wt.%.

ing the operation of the condenser outside the system box. These findings indicate that the overall system is nearly water-balanced, enabling it to operate without an external water supply.

The start-up time is another significant factor for commercialization of a portable DMFC. If the system is started up quickly, then the DMFC can be used without delay, and the system size can also be reduced by using a smaller start-up lithium battery. The start-up time depends on the initial methanol concentration, cell number stacked, loading situation, fuel and air flow rate. For instance, as shown in Fig. 9, the start-up time was reduced from 25 min (using 1 wt.% methanol solution) to 10 min (using 9 wt.% methanol solution as initial methanol concentration). The start-up time of our DMFC system was further decreased to less than 5 min by choosing the appropriate control parameters, as demonstrated in Fig. 10.

3.4. System performance analysis

In the process of system performance analysis, first, we use the DVD player for the real load to test the stability of the integrated system. Then we test our portable DMFC system performance with the notebook PC.

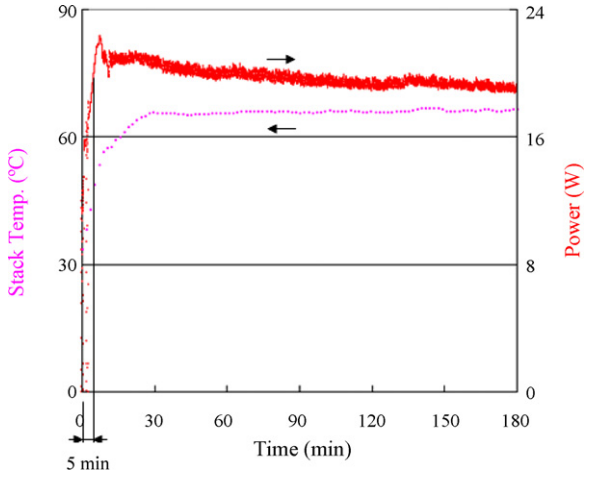

Fig. 10. Start-up characteristics of our DMFC system.

3.4.1. DVD test mode

Fig. 11 shows the DMFC system performance including the output power, the cell temperature and the battery power (for start-up) when we use the DVD player as the real load. The DMFC system is operated with methanol sensor-less control under two different situations using long and short fuel injection delay time (Mode 1 and Mode 2, respectively). Compare

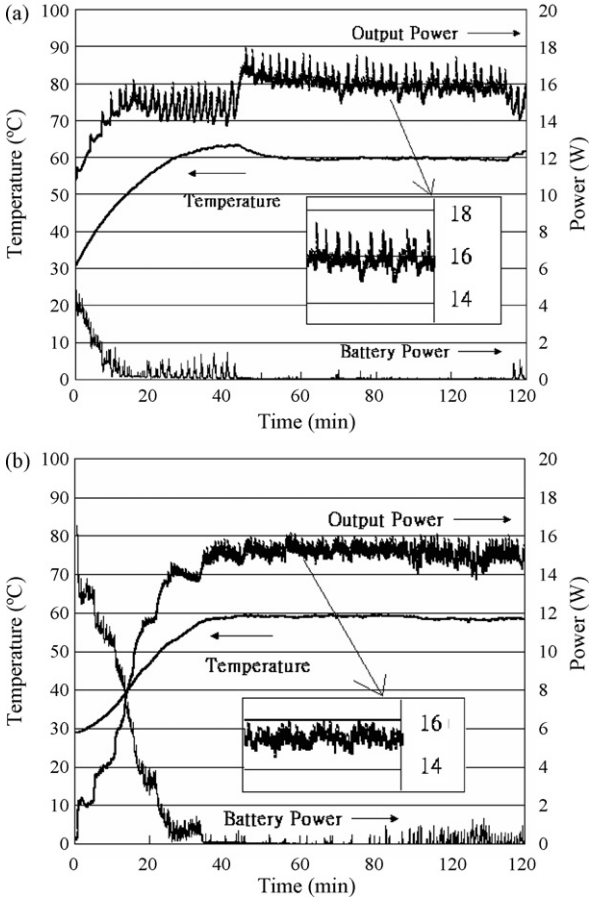

Fig. 11. The DMFC system performance with methanol sensor-less control for the DVD player operated under two different situations: (a) long fuel injection delay time; (b) short fuel injection delay time.

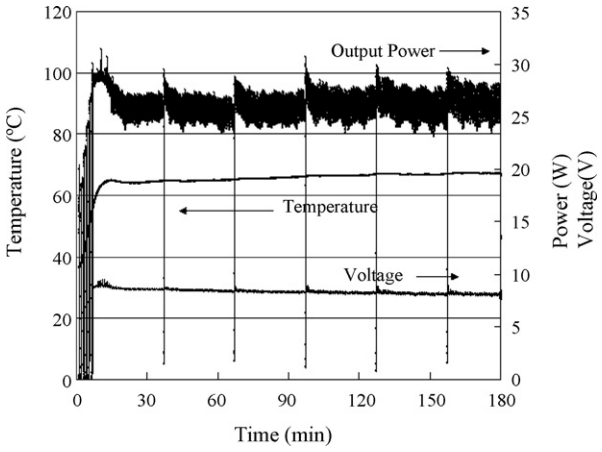

Fig. 12. The 3-h stability test of stack performance for notebook PC.

Fig. 11(a with b) for average power performance of 15–16 W, the output power fluctuation for Mode 1 and Mode 2 are 10 and 5%, respectively. It is shown that the shorter fuel injection delay time can reduce the generated power fluctuation, and promote the stability of the system.

3.4.2. Notebook PC test mode

After successful tests of using the DVD player as the real load, we take the notebook PC as the load to examine the performance and stability of the DMFC power pack system. Fig. 12 shows the 3-h stability test of the stack performance for notebook PC. The stack can output about 28 W steadily, and the power fluctuation is about ±7.7%. Fig. 13 shows a notebook PC powered by a portable DMFC system with an average net power of about 20 W.

During the short-term test with 3 h operation delivering 60 Wh of energy, we can calculated some important parameters, such as system energy density, balance of plant (BOP) efficiency, fuel efficiency and total efficiency of the system, to characterize the system performance. The BOP efficiency is defined as the ratio of net power output (P_{net}) to gross power output (P_{gross}) from the fuel cell. First, the power from the fuel cell must be conditioned to the desired voltage before the load device and any auxiliaries in the system, such as pumps, control circuits, etc. can be used. Part of the conditioned power is provided to the system auxiliaries to support fuel cell system operation. The

Fig. 13. A notebook PC powered by a portable DMFC system.

BOP efficiency, η_{BOP}, is obtained as

$$\eta_{BOP} = \frac{P_{net}}{P_{gross}} = \frac{(P_{gross} \times \eta_{DC-DC}) - P_{aux}}{P_{gross}}$$

where P_{aux} is the auxiliary power, η_{DC-DC} the DC–DC converter efficiency, and η_{BOP} is the function of the DC–DC converter efficiency, auxiliary power and gross power. The auxiliary power includes all power consumption by the system except the DC–DC converter for user's device. In our DMFC power pack system, these components including liquid and air pumps, control circuits, etc. use a total of ~6 W. The DC–DC converter efficiency of 92% is used in our DMFC system so that the BOP efficiency (η_{BOP}) is calculated to be about 71%. It means that 29% of the power generated by the fuel cell is used to support the BOP system operation.

Another important factor to value the system performance is the total efficiency of the system. The total efficiency is defined as the ratio of the electrical energy available for use to the chemical energy consumed. During net output of ~20 W (28 W × 0.71) to an external source (for notebook PC), the BOP requires ~6 W to support the fuel cell operation. The run time that the fuel cell provided power output was 3 h. Since the average net power output from the fuel cell is about 20 W, total energy produced is 3 h × 20 W = 60 Wh. Since the system used about 84 ml of pure methanol fuel during the test, the available energy is 401.5 Wh (0.084 L × 4780 Wh L^{-1}) as the methanol volumetric energy density is 4780 Wh L^{-1}. Therefore, overall total system efficiency (η_{system}) are determined as about 15% (100% × 60/401.5). The fuel efficiency (η_{FUEL}) can also be calculated from the system, BOP and load efficiency. Their relationship is given as:

$$\eta_{system} = \eta_{LOAD} \times \eta_{FUEL} \times \eta_{BOP}$$

where η_{LOAD} is a load efficiency defined as the ratio of the cell voltage to the thermoneutral voltage which is almost equal to theoretical open circuit voltage in the DMFC reaction. Therefore, the load efficiency is about 29% in the current DMFC system and the fuel efficiency (η_{FUEL}), which is also called the mass efficiency, is obtained as ~73%.

The energy density of the system depends on the volume, weight and net energy output of the system without refuel. The cartridge capacity is 300 mL with 200 mL of pure methanol fuel and can make sure the DMFC system is operated for about 8 h. So the total energy for 8-h operation is about 160 Wh (20 × 8 = 160 Wh) for 20 W system. Because the size and weight of the system (including cartridge) is 2.7 L and 2.72 kg, respectively, the system energy density is 59.3 Wh L^{-1} and the specific energy is 58.8 Wh kg^{-1}. For longer operation time, the system size remains the same and only fuel supply is needed. The 20 W system for 3 days (72 h) operation, 1.6 L of fuel would be required and the system will has 3.98 kg and 4.3 L. Therefore, when delivering energy of 1440 Wh, the system energy density for 72 h operation would be 335 Wh L^{-1} and the specific energy would be 362 Wh kg^{-1}, which are greater than those of lithium ion battery (~250 Wh L^{-1} and ~150 Wh kg^{-1}). Obviously, the DMFC system can reach commercial viability when compared to battery system for extended operation.

4. Conclusions

This work describes the proposed method for developing a 20 W DMFC power source for portable electronics. The study has demonstrated that a portable DMFC can be made by the system integration of key components, considering the effect of some technical issues, such as stack and condenser, methanol sensor-less control and start-up properties. The development of the portable system includes several improvements, including water balance and quick start-up. The overall system can be nearly water-balanced, allowing it to operate without an external water supply. The use of appropriate control parameters can reduce the start-up time of the DMFC system to below 5 min. For 3 days of operation, the system energy density is 335 Wh L^{-1}, and the specific energy is 362 Wh kg^{-1}, which are greater than the values for lithium batteries. Therefore, the DMFC is a good choice for next-generation power sources for portable application in electronics. Significantly, the portable system using the in situ mixing method with injection of pure methanol is demonstrated to power a DVD player and a notebook PC. The methanol sensor-less control algorithm can control the methanol concentration in the range 0.7–1.2%, resulting in a good fuel efficiency of 73% because of the reduction in methanol crossover. A methanol sensor-less control fuel cell system can hopefully improve portable DMFC systems for 3C applications due to its benefits of improved fuel efficiency, durability, miniaturization and cost reduction.

Acknowledgement

The authors would like to thank the Institute of Nuclear Energy Research (INER) of the Republic of China, Taiwan for financially supporting this research.

References

[1] W. Vielstich, A. Lamm, in: A.H. Gasteiger (Ed.), Handbook of Fuel Cells, John Wiley & Sons Ltd., England, 2003.
[2] J.M. Ogden, M.M. Steinbugler, T.G. Kreutz, J. Power Sources 79 (1999) 143–168.
[3] H. Chang, J.R. Kim, J.H. Cho, H.K. Kim, K.H. Choi, Solid State Ionics 148 (2002) 601–606.
[4] S.J.C. Cleghorn, S. Ren, T.E. Springler, M.S. Wilson, C. Zawodzinsky, T.A. Zawodzinscky, S. Gottesfeld, Int. J. Hydrogen Energy 22 (1997) 1137–1144.
[5] C.Y. Chen, C.S. Tsao, Int. J. Hydrogen Energy 31 (2006) 391–398.
[6] D. Kim, E.A. Cho, S.-A. Hong, I.-H. Oh, H.Y. Ha, J. Power Sources 130 (2004) 172–177.
[7] C.Y. Chen, P. Yang, J. Power Sources 123 (2003) 37–42.
[8] D. Kim, J. Lee, T.H. Lim, I.H. Oh, H.Y. Ha, J. Power Sources 155 (2006) 203–212.
[9] M. Broussely, G. Archdale, J. Power Sources 136 (2004) 386–394.
[10] A.S. Arico, P. Creti, V. Baglio, E. Modica, V. Antonucci, J. Power Sources 91 (2) (2000) 202–209.
[11] J.A. Drake, W. Wilson, K. Killeen, J. Electrochem. Soc. 151 (3) (2004) A413–A417.
[12] S.A. Ma, M. Odgaard, E. Skou, Solid State Ionics 176 (39/40) (2005) 2923–2927.
[13] F.Q. Liu, G.Q. Lu, C.Y. Wang, J. Electrochem. Soc. 153 (3) (2006) A543–A553.
[14] H. Dohle, J. Mergel, D. Stolten, J. Power Sources 111 (2002) 268–282.
[15] X.M. Ren, T.E. Springer, T.A. Zawodzinski, S. Gottesfeld, J. Electrochem. Soc. 147 (2000) 466–474.
[16] R.Z. Jiang, D. Chu, Electrochem. Solid-State Lett. 5 (7) (2002) A156–A159.
[17] R.Z. Jiang, C. Rong, D. n Chu, J. Power Sources 126 (2004) 119–124.
[18] H. Zhao, J. Shen, J. Zhang, H. Wang, D.P. Wilkinson, C. Elton Gu, J. Power Sources 117 (2006) 22–25.
[19] P.L. Antonucci, A.S. Arico, P. Creti, E. Ramunni, V. Antonucci, Solid State Ionics 125 (1999) 431–437.
[20] J.A. Kerres, J. Membr. Sci. 185 (2001) 3–27.
[21] H.S. Liu, C.J. Song, L. Zhang, J.J. Zhang, H.J. Wang, D.P. Wilkinson, J. Power Sources 155 (2006) 95–110.
[22] M. Gotz, H. Wendt, Electrochim. Acta 43 (1998) 3637–3644.
[23] C.Y. Chen, P. Yang, Y.S. Lee, K.F. Lin, J. Power Sources 141 (2005) 24–29.
[24] C.Y. Chen, J.Y. Shiu, Y.S. Lee, J. Power Sources 159 (2006) 1042–1047.
[25] C. Xie, J. Bostaph, J. Pavio, J. Power Sources 136 (2004) 55–65.
[26] C.L. Chang, C.Y. Chen, C.C. Sung, D.H. Liou, J. Power Sources 164 (2007) 606–613.